# Magnetically-Targeted, Technetium 99m-Labeled Nanoparticles to the Inner Ear

K. J. Dormer[1,*], V. Awasthi[3], W. Galbraith[3], R. D. Kopke[2], K. Chen[2], and R. Wassel[2]

[1] *Department of Physiology, University of Oklahoma Health Sciences Center, Oklahoma City, OK 73104, USA*
[2] *Hough Ear Institute, Oklahoma City, OK 73112, USA*
[3] *Department of Pharmaceutical Sciences, University of Oklahoma Health Sciences Center, Oklahoma City, OK 73117, USA*

The cochlea presents a hurdle for intravascular drug therapy because of the blood-labyrinthine barrier that tends to exclude entry of large molecules from its vasculature. Magnetic targeting of nanospheres through the cochlear round window membrane (RWM) may provide an entry for delivery of bioactive molecules for protection against or amelioration of acute sensorineural hearing loss. Multiple magnetite ($Fe_3O_4$) nanoparticles were encapsulated in biodegradable Poly(D,L-lactide-co-glycolide) (PLGA) providing high magnetic susceptibility and encapsulation of therapeutic payloads. These nanocomposites (MFNP) can be magnetically pulled through the RWM, enhance MRI and deliver payloads. It is important for pharmacokinetics to define the amounts of MFNP deliverable over time, under specific magnetic conditions. Hence, MFNP were conjugated with $^{99m}$Tc and solutions placed on the RWM of anesthetized guinea pigs ($n = 7$). The RWM was parallel to the pole face of an external magnet, experimental ear up, for 45 minutes. Control animals ($n = 7$) were tested with the same solution, without magnets. Following euthanasia, the cochlear perilymph was aspirated and soft tissues collected for gamma scintigraphy. Significantly more MFNP were pulled into the cochlea by magnetic targeting in this preliminary study, 330% above controls. Calculations of quantitative delivery were performed such that if individual therapeutic molecular loading was known, delivery of drugs could be calculated. We conclude that magnetic targeting to the cochlea across the RWM is a viable means of therapeutic delivery.

**Keywords:** Nanoparticle, PLGA, Cochlea, Magnetic, Technetium, Radionuclide.

## 1. INTRODUCTION

Deafness affects more than 30 million Americans and over 75% of hearing loss is attributed to sensorineural impairments. Worldwide there are estimated to be over 160 million persons with moderate to severe hearing loss (World Health Organization). Aging and occupational noise exposures are the leading causes of sensorineural hearing loss (SNHL), accounting for approximately 40% of the cases.[1] According to the National Institutes of Health, about one-third of Americans over age 60 have lost enough hearing to affect their understanding of conversational speech. Other causes of hearing loss include aminoglycoside antibiotics, certain chemotherapeutic drugs, infection, trauma, genetic, and congenital anomalies. Deafness is also the most common birth defect in the US, affecting 4 in 1000 live births annually. Most causes of SNHL involve loss of sensory hair cells and or auditory neurons over time through injurious processes of oxidative stress, inflammation and apoptosis. Therefore, rapid and timely delivery of therapeutic levels of anti-oxidants, protective neurotrophic factors, restorative plasmid DNA or interfering siRNA would be a beneficial treatment for protecting and treating the inner ear and balance organs. Oral or parenteral administration of therapeutic agents for inner ear disease or damage is complicated because of the blood-labyrinthine barrier (tight junctions between endothelial cells), low circulatory distribution to the cochlea, as well as, inherent problems of protein and DNA delivery by intravascular administration. Only about 1 in 100,000 molecules of a drug reach its intended target cell when administered by oral or parenteral means. Avoidance of systemic drug treatment side effects is desirable, hence, topical cochlear applications are currently being introduced clinically.[2] In the future, magnetic targeting of nanoparticles delivering therapeutic substances across the Round Window Membrane (RWM) into the cochlea might become a clinical tool in light of recent advances in both magnetics and nanoparticle technology.[3, 4]

---

*Author to whom correspondence should be addressed.

Magnetic nanoparticles (<100 nm) susceptible an external magnetic field, were first tested in animals in 1996 and are actively being studied for magnetic targeting of drug delivery, for hyperthermic tumor ablation and for contrast enhancement in MRI.[3–5] In addition to tissue targeting capabilities, the advantages of magnetically susceptible nanoparticles include their:

(a) ability to be guided or held in place by means of a magnetic field;

(b) enhanced localization by MRI;

(c) reduced drug use and cost;

(d) fewer side effects and low toxicity-teratogenicity-mutagenicity.[6]

Especially noteworthy in targeting the inner ear is avoidance of barriers imposed with vascular administration, such as scavenging by macrophages of the mononuclear phagocyte system.[7] Disadvantages of superparamagnetic nanoparticles include the need for a strong and localized magnetic field and gradient to target the particles *in vivo*. Ferrite nanoparticles such as magnetite ($Fe_3O_4$) are biocompatible since iron is a nutrient and readily metabolized by cellular regulation using the transferrin pathway and their ease of passing in and out of cells across the plasma membrane. By transporting through the RWM, nanospheres can deliver therapeutic payloads into cochlear perilymph, readily accessing both the organ of Corti and vestibular balance organs. We have pulled polymeric nanospheres through the RWM and into the cochleae of both rodent (*in vivo*) and human (*ex vivo*) labeled with coumarin-6 and encapsulating superparamagnetic iron oxide nanoparticles (SPION; magnetite).[8]

The RWM has been previously utilized as a small molecule, drug delivery portal to the inner ear for several years. Corticosteroids and more recently aminoglycoside antibiotics have been placed through the ear drum into the middle ear cavity, accessing the RWM, to treat a variety of disorders of hearing and balance.[9] This treatment approach has had a limited level of success and does not provide accurate inner ear dosing. Additionally, natural RWM permeability to larger molecules such as proteins and plasmid DNA is limited and variable for all drugs because of molecular size variations. Nevertheless, a variety of small molecules has been topically placed on the RWM of rodents, which diffused or transported into the cochlea and successfully treated noise-induced hearing loss and ototoxicity. Tamura[10] first showed PLGA naturally transporting a molecular payload (rhodamine dye) across the RWM and targeting the cochlea, more effectively than by systemic injection. Our approach, magnetic targeting, has the advantages of avoiding an opening into the inner ear, enhancing RWM transport of both large and small molecules, with potentially increased accuracy of dosing and efficacy of drugs.

Distribution of nanoparticles in a biological milieu can be quantified by radioactive labeling and tracing.[11] As such, Technetium-99m ($^{99m}Tc$) is a good label because of its high photon flux, optimal decay half-life and a relatively benign gamma ray emission of 140 KeV. Labeling of nanoparticles with $^{99m}Tc$ can be conveniently performed by stannous-based reduction.[12] However, it may be necessary to ensure stability of $^{99m}Tc$ 1 and to eliminate confounding colloidal tin oxide for proper interpretation of distribution kinetics.[13] The present study represents the first $^{99m}Tc$-labeled polymeric, magnetically susceptible SPION nanocomposite application, proving enhanced and quantifiable delivery for treatment of the inner ear. We formulated and tested *in vivo*, PLGA-magnetite-$^{99m}Tc$-labeled nanocomposites (175 nm, hydrodynamic diameter) as a platform for magnetic targeting of therapeutic substances to the inner ear. This multifunctional nanocomposite (MFNP) contains SPION (~12 nm) that render the MFNP susceptible to an external magnetic field for pulling through cell membranes and targeting tissues. Using gamma scintigraphy, anesthetized guinea pigs were used to quantify MFNP targeted into the cochlea across the RWM. The tympanic bulla was opened, exposing the round window membrane (RWM), and each animal positioned to align the RWM parallel to the pole face of a NeFeB permanent magnet. A 2 $\mu l$ solution of $^{99m}Tc$-labeled MFNP was placed in the niche of the RWM and allowed to remain for 45 minutes, whereupon cochlear tissues were dissected and harvested for gamma scintigraphy. Radioactivity from cochleae where MFNP solutions had been placed on the RWM was compared for magnetic targeting and control (no magnet) to determine if magnetic forces delivered more particles than diffusion and active transport. We found statistically higher gamma counts/min in the cochleae of experimental animals when compared to controls.

## 2. MATERIALS AND METHODS

### 2.1. Chemicals and Animal Model

Poly(D,L-lactide-co-glycolide) (50:50: lactide/glycolide, 1.13 dL/g viscosity) was purchased from Absorbable Polymers International (Pelham , AL). Poly-vinyl alcohol PVA (Mw 30–70 kDa) was purchased from Sigma Chemical Co. (St. Louis, MO). Iron oxide (magnetite) nanoparticles with oleic acid coating were purchased from Liquid Research LTD (Bangor, Gwenedd. LL527 2UP, UK). Chloroform (HPLC grade) was purchased from VWR (West Chester, PA). Tin(II) Chloride dihydrate, 98% ACS and sodium pertechnetate were purchased from Sigma-Aldrich (St. Louis, MO). Hydrochloric Acid 12.1 N was purchased from Fisher Scientific (Fair Lawn, NJ). Nitrogen was purchased from Airgas (Oklahoma City, OK). Technetium was acquired from a $^{99}$molybdenum/$^{99m}$technetium generator purchased from Bristol-Myers Squibb (Billerica, MA). PD-10 desalting column pre-packed with Sephadex™ G-25 was purchased from GE Healthcare (Piscataway, NJ).

ITLC-silica gel was purchased from VWR International (West Chester, PA).

Young adult, domestic, guinea pigs (*Cavia porcellus*; Hartley strain; Charles River Labs, Wilmington, MA) of either sex, weighing 300–350 gm, were selected for this study. The guinea pig has been a model for auditory studies because of the large middle ear space and surgical accessibility to the cochlea. The RWM, about 1 mm diameter, is accessible for placement of MFNP solutions carrying therapeutic molecules, some of which can diffuse readily across this three-layered membrane into the perilymphatic fluid of the inner ear. Crossing the RWM gives access to the organ of Corti, which contains the auditory hair cells, the transducers of hearing. Loss of these hair cells is the cause of sensorineural deafness. Experiments conducted were in protocol approved for K.D. by the University of Oklahoma Health Sciences Center Institutional Animal Care and Use Committee (IACUC) and we followed the Public Health Service Policy on Humane Care and use of Laboratory Animals.

## 2.2. Nanoparticle Synthesis

PLGA nanoparticles were synthesized using the double emulsion chloroform solvent evaporation technique.[14] The desired concentration of SPION (5.0 mg/ml) was dispersed into 1 ml of chloroform, and then 30 mg of PLGA was dissolved in the solution. Next, 200 $\mu$l of nanopure water (D-Q3 System, Millipore, Burlington, MA) was emulsified into the PLGA/SPION/chloroform solution for 1 min in an ice bath using a probe sonicator (Sonicator 2000, Misonix, NY) to form a water-in-oil emulsion. This primary emulsion was emulsified again by adding the water-in-oil emulsion 6 ml of nanopure water containing 2% polyvinyl alcohol (PVA). The system was sonicated for 5 minutes and stirred for ~24 hours to allow the chloroform to evaporate. The PLGA particles containing SPION were then recovered by centrifugation at 20,000 rpm for 25 min at 4 °C (Beckman Optima LE-90K, Beckman Instruments Inc, Palo Alto, CA). The particles were washed with nanopure water 4 times to remove any excess PVA and SPION and then dispersed in 1 ml of nanopure water in 2 ml cryotubes. The multifunctional PLGA-magnetite nanoparticles, MFNP, were then lyophilized for 2 days and stored in a desiccator at −20 °C until use in experiments. They remained stable for 8–10 months.

## 2.3. Radiolabeling and Purification

A modified stannous-based reduction method was used to radiolabel the MFNP with $^{99m}$Tc.[12] Technetium-99m as sodium pertechnetate (~50 mCi/ml) was produced from a technetium generator (Bristol-Myers Squibb, TechneLite®; Nuclear Pharmacy, OUHSC, Oklahoma City, OK). Quality control on the "fresh" generator eluate was performed as per the USP/NF standards. To label nanoparticles with $^{99m}$Tc, about 500 $\mu$l suspension of nanoparticles (12 mg/ml in nanopure water) was added to pertechnetate containing about 0.36 mg stannous chloride dihydrate. To uniformly suspend the MFNP, the suspension was sonicated using a probe sonicator (Microson XL 2000, Misonix Inc., Farmingdale, NY) for 15 seconds at 3 watts. The mixture was incubated at room temperature for 5 minutes, before applying it on a PD-10 desalting column (GE Healthcare, Piscataway, NJ) which had been previously washed with 3 column volumes of deionized water. Aliquots were collected and fractions containing majority of $^{99m}$Tc-nanoparticles were pooled together. To ensure $^{99m}$Tc labeling efficiency that was $84\pm9\%$, thin layer chromatography (ITLC-SG, VWR International, West Chester, PA) was performed with a 2 $\mu$l sample using 0.9% saline. The $^{99m}$Tc-nanoparticles remained at the point of application whereas free $^{99m}$Tc-pertechnetate traveled with the solvent front. A sample of $^{99m}$Tc-nanoparticles was routinely exposed to a magnetic field (2.7 Kgauss, Engineered Concepts, Birmingham, AL) to investigate the potential contamination of labeled nanoparticles with $^{99m}$Tc-stannous colloid. Magnetite nanoparticles clearly formed a pellet near the magnet, leaving any free of colloidal non-magnetic radioactivity in suspension. The supernatant and the nanoparticle pellet were counted for $^{99m}$Tc radioactivity.

## 2.4. Nanoparticle Characterization

Dynamic Light Scattering (DLS) and zeta potential measurements in water were performed to determine PLGA particle (hydrodynamic) size and surface potential, respectively (Brookhaven Zeta PALS, Long Island, NY). Transmission electron micrographs (TEM) were taken also to determine particle size and the qualitative state of aggregation of the SPION inside the PLGA particles (H7600 Electron Microscope, Hitachi, Pleasanton, CA). For TEM images, a drop of the MFNP was placed on a formvar-coated copper grid. Magnetization measurements were performed at room temperature using a vibrating sample magnetometer (Lakeshore Cryotronics Inc., Westerville, OH).

## 2.5. Animal Surgery and Magnetic Targeting

Guinea pigs were anesthetized using ketamine HCL (Phoenix Scientific Inc., St. Joseph, MO; 60 mg/kg i.m.) and xylazine (Phoenix Scientific Inc., St Joseph, MO; 6 mg/kg i.m.) and the hair clipped behind the ear. Using aseptic technique, a post-auricular skin incision was made to expose the right auditory bulla. Skin bleeding was minimized using lidocaine with 1% epinephrine (Hospira Inc., Lake Forest, IL; 0.5 ml, s.c.). Under an operating microscope (Zeiss Inc., Zurich, OPMI 1) the tympanic bulla was opened, exposing the middle ear cavity and niche of the Round Window Membrane (RWM).

RESEARCH ARTICLE

In preliminary experiments, the horizontal plane of the RWM had been positioned with respect to an underlying permanent magnet ($4 \times 4 \times 4$ inches,, NdFeB, Integrated Magnetics, Culver City, CA) using a laser triangulation sensor (MTI Instruments, Inc., Albany, NY; Model Microtrak II; spot size 20 $\mu$m; distance sensitivity 20 $\mu$m). It is important for optimal magnetic targeting that the RWM be positioned perpendicular to the lines of flux in the external magnetic field, parallel to the pole face of the magnet. The guinea pigs were placed on their left sides on an adjustable plastic base with a head positioner, where the angles of left-right head rotation and up-down head elevation were controllable. This rodent cochlear RWM positioning apparatus is diagrammed in Figure 1. Angles of the head were changed while precise distances from the laser sensor were recorded so as to establish equal distances to the perimeter of the RWM. Thus, rotation and elevation of the head positioned the RWM, parallel to the pole face of the magnet. Equal distances meant the plane of the RWM was horizontal. This resulting head position was noted and used for all subsequent magnetic targeting experiments.

Once the RWM was horizontally positioned, 2 $\mu$l of $^{99m}$Tc labeled MFNP solution (0.2 mg/ml) was injected onto the surface of the RWM in the right ear using a 10 $\mu$l syringe (Hamilton Co., Reno, NV). Three groups of animals were tested, with experimental (magnetic field) and control (no magnetic field) animals randomized in the respective groups. Experimental animals ($n = 7$ total) were exposed to approximately 2.5 Kgauss for 45 minutes, while control animals ($n = 7$ total) were identically tested. The residual nanoparticle solution was wicked off the RWM at the end of 45 min using tissue paper that was saved in a scintillation vial for gamma counting of radioactivity that did not enter the cochlea. Next, each animal received an intracardiac injection of euthanasia solution

(Pentobarbital sodium, 2 grains, Anpro Pharmaceuticals, Arcadia, CA). The temporal bones were dissected from the head and cochleae isolated. Special attention was given to avoid damaging the stapes and RWM. The operated cochleae were positioned apex upward for dissection, beginning with a small hole picked at the apex. Cochlear perilymph was wicked through the hole using paper wicks that were saved for gamma scintigraphy of counts/min from MFNP targeted into the cochlea. Cochlear bony wall was progressively removed by rongeur, one turn at a time, while the soft tissue (stria vascularis, basilar membrane, spiral ligament, spiral ganglion) was progressively removed along with perilymph. These soft tissues and perilymph were saved for gamma scintigraphy of MFNP targeted into the cochlea. Dissection was completed at the basal turn with the RWM left intact. The boney wall chips and cochleae with attached RWM were saved for gamma scintigraphy and counts/min of MFNP not targeted into the cochleae. One ml water was added to each scintillation vial to equally position the paper wicks in the window of the gamma counter (Cobra II, Perkin-Elmer, Waltham, MA).

Scintigraphy separated the targeted and non-targeted $^{99m}$Tc-labeled MFNP into gamma counts/min inside or outside of the cochleae, respectively. Absolute gamma emissions and percent of total were recorded. An additional control for mass balance ($n = 3$ per experiment) was measured where a separate 2 $\mu$l sample of the $^{99m}$Tc-labeled MFNP solution was saved and counts/min recorded.

Knowing percent labeling of nanoparticles with $^{99m}$Tc and the weight of the nanoparticles after labeling we calculated the amount of $^{99m}$Tc-nanoparticles targeted from each 2 $\mu$l application to the RWM, by using the following equations:

Weight of NPs in 2 $\mu$l application

$$= \left( \frac{\text{starting weight of NP after TC}^{99m} \text{ labeling}}{\text{volume of solution}} \right) \times 2 \ \mu l \quad (1)$$

Weight of NPs that pass through the RWM

$$= \% \text{ NP in cochlea} \times \text{Weight of NPs in 2 } \mu l \text{ dose} \quad (2)$$

Once the weight of the nanoparticles that have passed through the RWM was calculated the concentration in $\mu$g/$\mu$l was derived by assuming that the volume of perilymph in the in a guinea pig cochlea is 4.76 $\mu$l. The number of particles that passed through the RWM was calculated by estimating the weight of one nanoparticle. The weight of one nanoparticle was estimated by using the following calculations.

$$\rho_{\text{NP}} = \left( \frac{1}{\left( \frac{\text{weight fraction of plga}}{\rho_{\text{PLGA}}} \right) + \left( \frac{\text{weight fraction of magnetite}}{\rho_{\text{magnetite}}} \right)} \right) \quad (3)$$
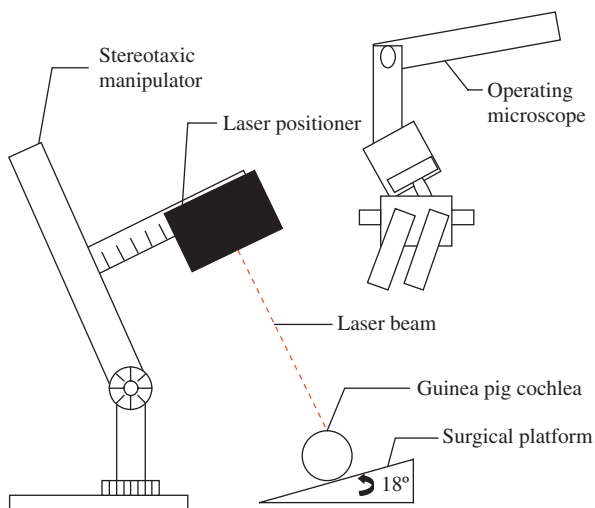


**Fig. 1.** Laser triangulation apparatus for horizontal positioning of the guinea pig round window membrane for surgical positioning and application of $^{99m}$Tc-labeled MFNP to the RWM.

Where $\rho_{NP}$ is the combined density of the PLGA and magnetite (gm/cm$^3$)

$$V_{NP} = \left( \pi \times \frac{4}{3} \times \text{NP radius via TEM} \right)^3 \qquad (4)$$

Where $V_{NP}$ is the theoretical volume of the nanoparticle (nm$^3$)

$$W_{np} = V_{NP} \times \rho_{NP} \times N_A \qquad (5)$$

Where $W_{np}$ is the theoretical weight of one nanoparticle (g/particle).

## 2.6. Statistical Analysis

The scintillation counts/min of targeted MFNP (internalized into cochlear perilymph and soft tissues) and nontargeted MFNP (residual, outside the RWM and within the RWM) were used to calculate the ratio of RWM transport. The mean $\pm$ standard error of counts/min from the experimental (magnet) and control (no magnet) groups were calculated, and compared using Student's Paired t-statistic (one-tailed). The significance level was set as $p < 0.05$ for 95% confidence. Using Eqs. (1–5), intracochlear concentration, number and mass were calculated and compared using Student's Paired t-statistic.

## 3. RESULTS

### 3.1. Characterization of PLGA-Magnetite Nanoparticles

Synthesis of the PLGA-magnetite nanocomposite was performed before conjugating with $^{99m}$Tc. Synthetic procedures followed the accepted published methods for water-oil-water double emulsion synthesis of PLGA nanoparticles. The MFNP, prior to $^{99m}$Tc conjugation, had a (hydrodynamic) diameter of 175 nm with a polydispersity index of 0.045 measured by dynamic light scattering (DLS). Using transmission electron microscopy (TEM), the oleic acid-coated superparamagnetic iron oxide nanoparticles (SPION) appeared to range in size from 5 to 15 nm, yet incorporation of these SPION did not influence the final size of the PLGA-magnetite particles. Figure 2 is a scanning electron micrograph (SEM) of the PLGA particle without $^{99m}$Tc labeling. Previously we had shown using TEM that the magnetite particles were only slightly aggregated within the PLGA, although this is difficult to determine since particles separated in the *z*-direction will appear aggregated in a two-dimensional view (Wassel, 2007). This slight aggregation is probably not an artifact of particle evaporation on the TEM grid since the oleic acid-coated, PLGA-encapsulated SPION were not freely mobile. Otherwise, SPION dispersion is very good, resulting in good magnetic susceptibility of the particles. When a lower concentration of magnetite was used (1 mg/ml vs. 5 mg/ml) in the synthesis of the PLGA-magnetite nanocomposite,
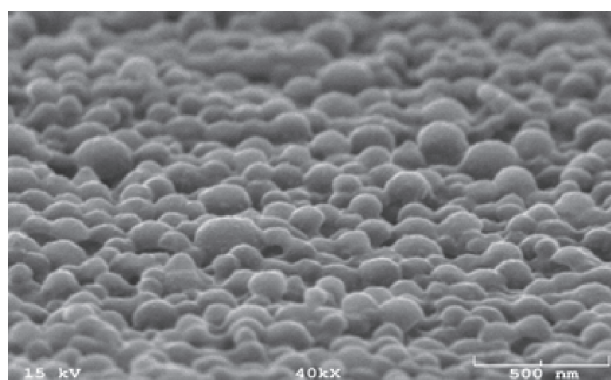


**Fig. 2.** SEM of PLGA nanoparticles used to incorporate magnetite and conjugate with $^{99m}$Tc.

fewer magnetite particles were incorporated into the polymer and their appeared to be no aggregation. There was no apparent relative partitioning of SPION in one PLGA particle compared with another, except for expected partitioning due to randomization. The weight percent of the magnetite was determined by burning the samples and measuring the mass remaining; lower concentrations could not be measured reliably with this method because of the small amount of magnetite in the PLGA particles. Approximately 50% of the magnetite suspended in chloroform was incorporated into the PLGA.[15] It can be seen in Figure 2 that the particles are spherical with occasional ellipsoidal shapes, which likely is due to warming and partial melting of the PLGA caused during SEM.

Particle magnetization curves are shown in Figure 3 for initial magnetite concentrations of 0, 0.1, 1.0, 5.0 and 10 mg/ml in the organic phase. Saturations are higher than
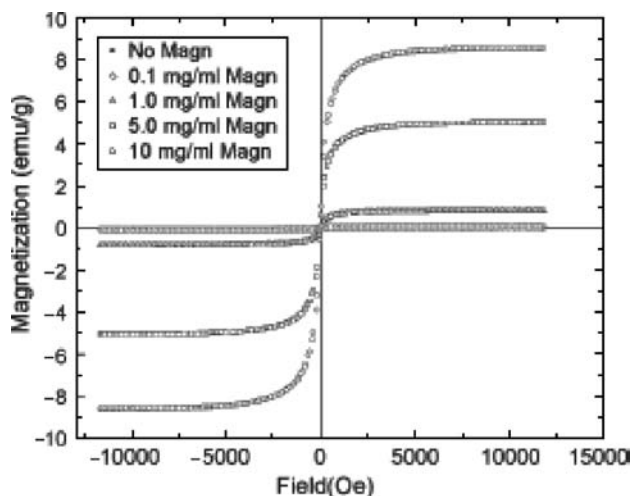


**Fig. 3.** Hysteresis curves for magnetization of PLGA microparticles with encapsulated magnetite. The different concentrations represent various initial concentrations of magnetite in the organic phase prior to emulsification. Reprinted with permission from [15], R. A. Wassel et al., Dispersion of superparamagnetic iron oxide nanoparticles in poly(D,L-lactide-co-glycolide) microparticles. *Colloids and Surfaces A: Physicochemical Eng. Aspects* 292, 125 (**2007**). © 2007.

reported by others. For example, using the same weight ratios, susceptibility of these particles is 70 emu/gm, compared with 50 emu/gm particles produced by Okassa.[16] These PLGA-magnetite particles are formulated to carry three types of therapeutic biomolecules: small molecules such as antioxidants, proteins and DNA/RNA. Because of the multiple roles of PLGA-magnetite in promoting endocytosis and endolysosomal escape, programmed biodegradation, different payload carrying capacities, magnetic susceptibility and enhanced MRI, we identified these as multifunctional nanoparticles (MFNP).

## 3.2. Radiolabeling

In order to follow the targeting potential of PLGA magnetite nanoparticles under magnetic field, we radiolabeled the nanocomposite preparation with $^{99m}$Tc and separated the labeled particles from free radioactivity in a Sephadex™ G-25 column. The labeling efficiency was $84 \pm 9\%$. As shown in the elution profile of the labeled preparation (Fig. 4), the $^{99m}$Tc-nanoparticles were clearly separated from free radioactivity. Labeled nanoparticles were eluted within 4 ml whereas free $^{99m}$Tc-pertechnetate eluted after 10 ml. Considering that the nanoparticle manufacturing process involved coating of magnetite particles with oleic acid before PLGA modification, additional control of oleic acid magnetite was also labeled with $^{99m}$Tc. Oleic acid magnetite particles also labeled with an efficiency of over more than 90%. Like PLGA nanoparticles, the labeled particles remain at the point application in silica gel TLC/0.9% saline system. However, when the solvent was changed from 0.9% saline to acetone, the radioactivity peak traveled with the solvent front, suggesting that the oleic acid magnetite particles were stripped-off of oleic acid coating by the organic solvent. The elution profile of $^{99m}$Tc-oleic acid magnetite particles in PD-10 column was entirely different from that of $^{99m}$Tc-PLGA nanoparticles.
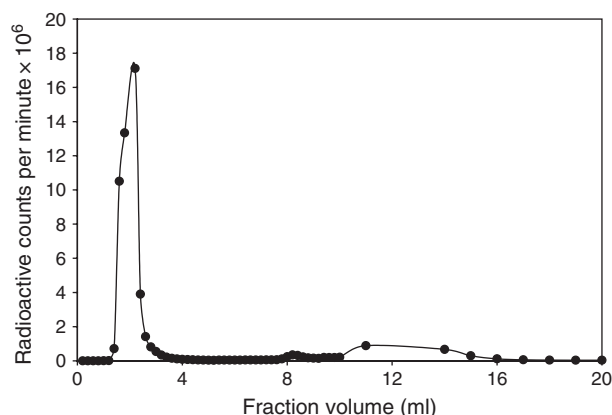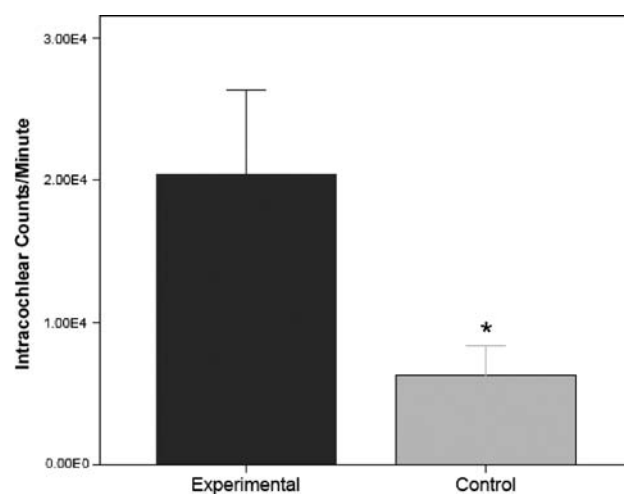
Technetium labeled oleic acid magnetite particles could not be eluted from the column even after six column volumes of elution medium.

To eliminate the possibility of $^{99m}$Tc-stannous colloid contamination in the preparation, an aliquot of $^{99m}$Tc-nanoparticles was placed under the influence of magnetic field for 1 h. There was clear separation of magnetite particles and supernatant, which upon counting, demonstrated that more than 95% of radioactivity was associated with the nanoparticle pellet. Technetium labeled stannous colloid, if present, was expected to stay in the supernatant. These experiments suggest that the PLGA nanoparticles can be stably labeled with $^{99m}$Tc in order to follow magnetic targeting in the inner ear following RWM administration.

## 3.3. Magnetic Targeting to the Cochlea

We developed this polymeric, magnetically susceptible, nanocomposite for use in delivering therapeutic moities to the inner ear. These MFNP can carry differing payloads for such treatments as either protection against injury to the sensory cells of the cochlea or amelioration from injury having occurred or restoration of sensory cells. Model small molecules, proteins and pDNA payloads have been incorporated into the PLGA. The purpose of this study, however, was to prove that magnetic targeting was superior to normal cellular mechanisms of transport across a live mammalian RWM into the cochlea. To confirm targeting, $^{99m}$Tc conjugated to the nanocomposite and gamma scintigraphy measurements enabled quantitative measurements of the PLGA-magnetite-$^{99m}$Tc targeted to the cochlea. In the three sets of experiments, with the $^{99m}$Tc-labeled nanocomposite recovered from outside and

**Fig. 4.** Sephadex™ G-25 column elution profile with $84 \pm 9\%$ $^{99m}$Tc-labeled MFNP activity collected in 2–3.8 ml fractions. $^{99m}$Tc-colloid activity collected after 8 ml and free $^{99m}$Tc-pertechnetate activity collected from 10–16 ml.

**Fig. 5.** Intracochlear gamma radioactivity (mean $\pm$ SEM, counts/min) from guinea pigs after 2 $\mu$l of $^{99m}$Tc-labeled-PLGA nanoparticles were placed on the guinea pig round window membrane, then exposed to either magnetic targeting ($n = 7$) or no magnet (control; $n = 7$) for 45 minutes ($P = 0.04$).
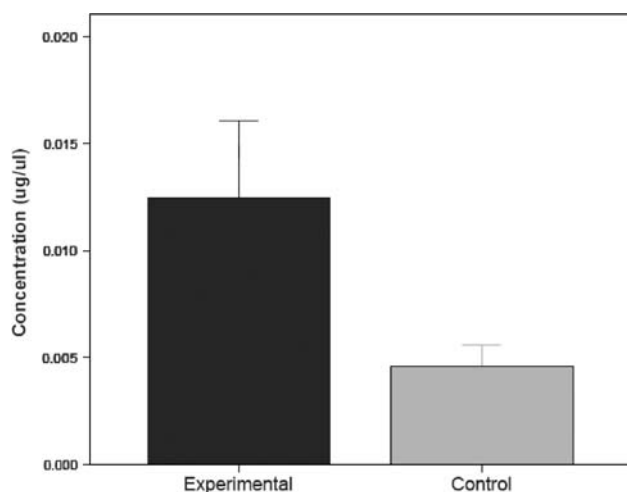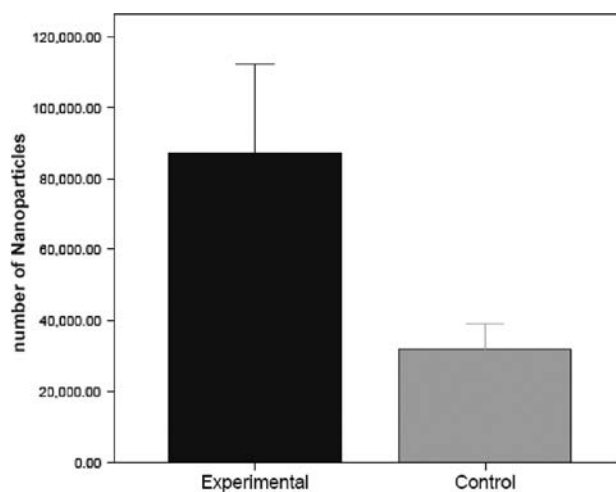
**Fig. 6.** Intracochlear concentration of $^{99m}$Tc-labeled-PLGA nano-particles (mean $\pm$ SEM $\mu$g/ml) in guinea pigs after 2 $\mu$l of was placed on the round window membrane ($p = 0.057$).

inside of the cochlea, there was an average of 81% recovery of the total dose placed on the RWM for the experimental animals ($n = 7$) and an average recovery of the total dose of 62% in the control series ($n = 7$), giving an overall average recovery of 72%. That is, an average of 28% of the 2 $\mu$l dose placed on the RWM was not accounted for in the sum of the counts/min (CPM) from inside plus outside the cochlea. Figure 5 shows the CPM of gamma activity from perilymph fluid and soft tissues within the cochlea in control animals compared with those cochleae exposed to 2.5 Kgauss. This represents a 330%, significant increase in MFNP internalization across the RWM over controls ($P = 0.04$).

Comparisons were also made using the mathematical conversions from CPM to intracochlear concentration, mass of MFNP targeted into the perilymph and intracochlear numbers of MFNP. These data are graphed in
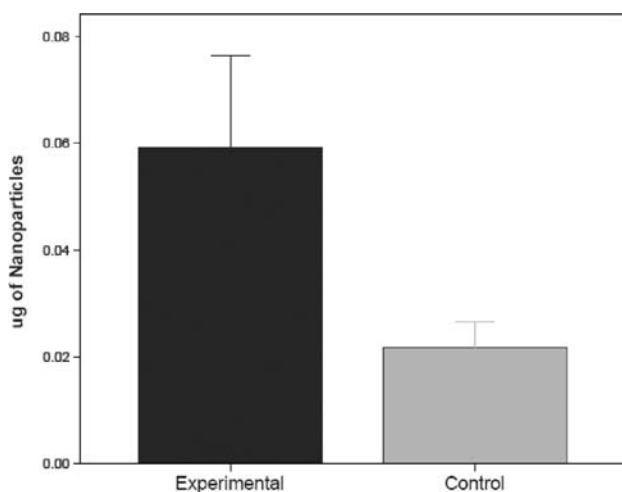


**Fig. 7.** Intracochlear mass of $^{99m}$Tc-labeled-PLGA nanoparticles in guinea pigs (mean $\pm$ SEM $\mu$g) after 2 $\mu$l of was placed on the round window membrane ($p = 0.057$).



**Fig. 8.** Intracochlear number of $^{99m}$Tc-labeled-PLGA nanoparticles in guinea pigs (mean $\pm$ SEM) after 2 $\mu$l of was placed on the round window membrane ($p = 0.057$).

Figures 6, 7 and 8, respectively. Although the clear trends for these data were identical with actual CPM, they were not statistically different ($P = 0.057$).

## 4. DISCUSSION

This study utilized $^{99m}$Tc as a tracer to verify that the combination of a PLGA nanoparticle, containing multiple, smaller superparamagnetic ($Fe_3O_4$) nanoparticles can enter the mammalian inner ear, passing through the RWM by attractive forces imposed by an external magnet. We concluded that transport of PLGA-magnetite-$^{99m}$Tc nanoparticles across the cochlear RWM was significantly greater than diffusion and active cellular transport alone. A multifunctional nanoparticle, one that can carry various payloads, including small molecules (e.g., antioxidants), neurotrophins (e.g., brain derived neurotrophic factor), pDNA (e.g., Math-1) or siRNA for magnetic targeting of therapeutic agents to the inner ear, and which enhances MRI, represents a potentially new nanomedicine regimen in otology. Because of the blood-labyrinthine vascular barrier, oral or intravenous medications have great difficulty achieving therapeutic levels in the cochlea. Thus, transmembrane targeting through the RWM into the cochlea may be an effective means to administer biomolecules or gene therapies. Important for magnetic targeting will be release pharmacokinetics. Hence, estimating the amount of drug delivered by MFNP is the first step in calculating release rates and dosing. The $^{99m}$Tc labeling provided quantitative measures of the numbers of PLGA-magnetite-$^{99m}$Tc nanoparticles delivered to perilymph and soft tissues of a mammalian cochlea. Knowing the efficiency of $^{99m}$Tc tagging, the numbers of particles targeted, the encapsulation efficiency of the MFNP for the respective payloads, and the release rate (biodegradation of the PLGA), one can begin to estimate timed doses of drugs or genes delivered

to the cochlea. Critical for non-viral gene therapy is the timed biodegradation of PLGA so that pDNA, for example, can transfect cells over days to weeks.

Important for effective magnetic targeting with this PLGA-magnetite composite was the relatively high magnetic susceptibility of the nanoparticles. This was attributable to good dispersion of SPION within the PLGA.[15] Others have subsequently reported on iron oxide encapsulation within PLGA, and with an average hydrodynamic diameter similar to ours at 280 nm but their magnetic susceptibility on a weight to weight basis was about half of the particles used in these experiments.[16]

The mechanism of magnetic targeting is not a new concept.[11] Magnetite in particulate sizes less than 20 nm displays superparamagnetism where single domain ferrite structures express dipoles only in the presence of an external magnetic field, yet have zero remanence in the absence of an external field. Magnetite SPION, encapsulated in PLGA retain their superparamagnetism, enabling magnetic targeting where particles are pulled through three cell layers of the RWM. Similar technology is available commercially for increasing non-viral transfection efficiency where magnetically-susceptible nanoparticle vectors are more effectively brought in contact with cell membranes *in vitro* (Magnetofection™). In magnetofection natural endocytosis internalizes nanoparticles across cell membranes.[17] For pulling nanoparticles through cells and membranes, we characterized the necessary forces on our MFNP[18] having proven they can be pulled through a tripartite RWM cell culture model[19] and subsequently across the RWM of guinea pigs and humans, fresh frozen cadaveric temporal bones.[8]

Ferrites as micro- or nanoparticles have been used for decades in biomedical applications but prior studies mostly used milled particles without the benefit of superparamagnetism and nanocomposites.[4, 7] Fundamental for membrane transport in the presence of a magnetic field, besides small size, is minimal agglomeration. Van der Waals forces will promote agglomeration if particles come into close proximity. High surface potentials tend to prevent but high magnetization tends to promote agglomeration. Hence, optimal magnetic targeting requires a balance between natural and induced forces so that individual particles and not agglomerations initially come in contact with the cell membrane.

There are numerous past and present endeavors using polymers in nanoparticulate drug delivery systems, the first pharmaceutical application reported in the 1970's.[20] Of the polymers and co-polymers such as PLGA, biocompatibility and biodegradability are key properties. We selected PLGA not only for its biocompatibility as the polymer most used worldwide in medicine but also for its propensity for endocytosis and escape from endolysosomes as has been demonstrated in non-viral gene therapy using PLGA as the vector. For example annexic

A2 is a membrane bound protein that is over-expressed in certain cancers. Down-regulation of annexin A2 was achieved using PLGA nanoparticles to deliver siRNA to metastatic prostate cancer cells.[21] With the PLGA encapsulation of oleate-magnetite, its size control (<200 nm) and its capability of carrying various therapeutic payloads, our MFNP is well suited for otologic applications.[8, 22]

Technetium labeling of nanoparticles has been used in numerous applications for tracking and therapy. Tracking of orally administered nanoparticles of 5-fluorouracil ^{125}I sodium alginate-bovine serum albumin elucidated the filtering and trapping of nanoparticles by liver, spleen and lungs.[23] The pharmacodynamics of polyethyleneglycol (PEG) encapsulated polylactic acid nanoparticles carrying protein was evaluated using a model antigen, ^{125}I labeled tetanus toxoid. Radionuclide tracing also showed that peglyation protected the nanoparticle payload from destruction by digestive fluids, revealing higher levels in blood stream and lymphatics.[24] Targeting of tumors by nanoparticles carrying radionuclides shows promise for both imaging and radiotherapy in cancer treatments. Micelles from amphiphilic diblock copolymers have been functionalized with folate and labeled with ^{64}Cu for ligand-receptor attachment to tumor cells. In spite of the usually excessive uptake of nanoparticles by the reticuloendothelial system, small tumors were treatable in mice.[25] Radioactive dirhenium decacarbonyl also has been loaded in poly (l-lactide) nanoparticles for intratumoral cancer therapy. Encapsulated in its crystalline natural state, the nanoparticle containing rhenium was rendered radioactive by bombardment with neutron flux.[26]

Technetium 99m has been used in a number of nanoparticle labeling applications, but no one has used ^{99m}Tc to quantify magnetic targeting as in the present study. The ^{99m}Tc-labeled Antimony sulfide colloid (<50 nm) and sulfur colloid (<200 nm) have been applied in cancer therapy to detect metastasis in lymph nodes.[27, 28] Nano-sized liposomes have been labeled with ^{99m}Tc in order to investigate their biodistribution and application in targeting inflammation and infection.[29] Magnetite labeled with ^{99m}Tc, when injected in rats intravenously, revealed by gamma photography the *in vivo* distribution of particles and that they could be magnetically restrained in anatomical targets.[30] In nasal drug delivery, mucocillary clearance was measured by ^{99m}Tc–PLGA microparticles and it was shown by gamma scintigraphy that 48.5% of the particles were cleared from the nose 4 hours after administration.[31] In chemotherapy, a major limitation of intravenous agents is their short lifetime before being scavenged by the mononuclear phagocyte system. Etoposide incorporated in tripalmitin nanoparticles was labeled with ^{99m}Tc for pharmacokinetic measurements and it was shown that positively charged particles had a higher circulation time and distribution in brain.[32] A recent imaging study by Zielhuis[33] showed that liposome nanoparticles, co-loaded with ^{99m}Tc and paramagnetic gadolinium, could

be used for both multimodality single-photon emission computed tomography (SPECT) and magnetic resonance imaging (MRI) and radionuclide therapy with one single agent. Yet another application of the use of ^{99m}Tc in tracking nanoparticle distribution *in vivo* may be in assessing nanoparticulate air pollution and translocation from lung to circulation. Inhaled ^{99m}Tc-labeled carbon nanoparticles (4–20 nm) have been found immediately in blood and gamma scintigraphy showed 95.6% retention in lungs after 6 h.[34] A non-invasive method for predicting the pretreatment tumor response to hyperthermia was shown in a rat model by using ^{99m}Tc-labeled liposomes to track and image their extravasations. By quantifying ^{99m}Tc-nanoparticle delivery to a tumor, the dose of chemotherapeutic Doxil could be better approximated.[35] Along similar lines, Park[36] applied ^{99m}Tc labeling and tracer technique to demonstrate that ionic-strength sensitive pullulan acetate nanoparticles had significantly longer rentention in a tumor bearing mice model when intratumorally administered.[36] Finally, as an extension of [99m]Tc *in vivo* imaging, distribution and kinetics, nanoparticles were adapted to deliver Rhenium-188-based particle radiotherapy. Employing the similar chemistry between ^{99m}Tc and [188]Re, it was proposed that [188]Re-labeled immuno-magnetic nanoparticle may be used in liver cancer treatment.[37]

A noteworthy experimental variable in this study was that CPM outside the cochlea after 45 minutes of magnetic targeting included the RWM. The bony cochlea with RWM and its ^{99m}Tc was considered as non-internalized nanoparticles. Realistically, those ^{99m}Tc-labeled MFNP within the RWM had already been captured by the magnetic field and were en route across the RWM into the perilymph. Hence, longer magnetic exposure time would likely have resulted in even greater percent internalization of the 2.0 $\mu$l dose of nanoparticle solution placed on the RWM. Related to physical forces, there is also the possibility that some of the MFNP exposed to the external magnetic field came into close proximity, agglomerated at the surface, and were not able to pass through the RWM into the perilymph of the scala tympani. Such quantification using scintigraphy is a limitation in the study because those particles in the RWM are not counted as having been transported. Nevertheless, in absolute counts, significantly greater internalization occurred.

One limitation of this study involves optimization of the magnetic field strength and gradient, which are physically responsible for the amount and rate of MFNP targeting across the RWM. The size, surface charge and magnetic susceptibility of the MFNP should be matched with parameters of the external magnetic field and gradient for optimal magnetic targeting. If the solution of MFNP placed on the RWM were to remain stable when subjected to the magnetic field, then as particles moved at the same velocity and with the same vector and were not slowed *en passage* through the RWM, then optimal targeting would take place. Another limitation arose because of synthetic and stochiometric constraints. The MFNP could not be loaded with both the respective payload and ^{99m}Tc simultaneously. Targeting data were based on the PLGA-magnetite-^{99m}Tc internalization. Thus, any predictions of actual rate of delivery and dose are made based on the PLGA-magnetite-^{99m}Tc transport data. Most likely, MFNP with therapeutic payloads will differ in sizes and surface charges, which will affect magnetic targetintg. Thirdly, the small volume of perilymph sampled along with a substantial number of the ^{99m}Tc-labeled particles remaining within the RWM and not counted as delivered into the cochlear fluid, lead to high variance in the means. Only 62–82% of the label placed on the RWM was recovered for analysis. Nevertheless, the measure of counts/min was significantly different between experimental and control animals.

The results of this tracing study support the overall goal toward magnetic targeting of the human cochlea. With the limitations of the guinea pig, smaller RWM size (area through which particles transport), less than optimal magnetic field and gradient, some agglomeration of particles on the surface of the RWM, there nevertheless was about 330% greater delivery by magnetic forces over diffusion and active transport across the RWM. We then can hypothesize that with further optimizations of particle size, morphology and magnetic susceptibility and with external magnetic forces matched to the MFNP, that targeting across the larger human RWM will be greater and more rapid. Indeed, in preliminary computerized axial tomography (CT) studies on a series of human temporal bones, we have calculated the geometries and distances from the skull surface to the RWM, suggesting that an external magnetic field placement for the human can replicate the results of these present studies. Magnetic stereotaxy is currently in use for anatomically interactive head and neck surgeries where magnetic fields, in conjunction with CT, guide surgical instruments. The interaction of an external magnetic field with middle and inner ear microanatomy is another prospective application of magnetic stereotaxy. Magnetic targeted delivery of therapeutic substances to the inner ear for protection against acute insults to hearing, for antibiotic rescue and for multifarious gene therapies that could be corrective to hearing loss are within the realm of possibility.

RESEARCH ARTICLE

Brian Grady, Ph.D. (University of Oklahoma, Norman, OK) in synthesis and loading of nanoparticles.

## References and Notes

1. D. J. Lee, O. Gomez-Martin, B. L. Lam, and D. D. Zheng, Trends in hearing impairment in United States adults: The national health interview survey, 1986–1995. *J. Gerontol.: Med. Sci.* 59A, 1186 (**2006**).

2. T. Endo, T. Nakagawa, T. Kita, F. Iguchi, T. S. Kim, T. Tamura, K. Iwai, Y. Tabata, and J. Ito, Novel strategy for treatment of inner ears using a biodegradable gel. *Laryngoscope* 115, 2016 (**2005**).

3. J. Dobson, Magnetic micro-and nano-particle based targeting for drug and gene delivery. *Nanomedicine* 1, 31 (**2006**).

4. D. Leslie-Pelecky, V. Labhasetwar, and R. H. Kraus, Advanced Magnetic Nanostructures, edited by D. J. Sellmyer and R. Skomski, Springer Publishing, New York (**2006**), pp. 461–490.

5. A. S. Lubbe et al., Preclinical experiences with magnetic drug targeting: Tolerance and efficiency. *Cancer Res.* 56, 4694 (**1996**).

6. Q. A. Pankhurst, J. Conoly, S. K. Jones, and J. Dobson, Applications of magnetic nanoparticles in biomedicine. *J. Phys. D: Appl. Phys.* 36, R167 (**2003**).

7. M. W. Freeman et al., Magnetism in medicine. *J. Appl. Phys.* 31, S404 (**1960**).

8. R. D. Kopke, R. A. Wassel, F. Mondalek, B. Grady, K. Chen, J. Liu, D. Gibson, and K. J. Dormer, Magnetic nanoparticles: Inner ear targeted molecular delivery and middle ear implant. *Audiol. Neurotol.* 11, 23 (**2006**).

9. R. D. Kopke, M. E. Hoffer, D. Wester, M. J. O'Leary, and R. L. Jackson, Targeted topical steroid therapy in sudden sensorineural hearing loss. *Otol. Neurotol.* 22, 475 (**2001**).

10. T. Tamura, T. Kita, T. Nakgawa, T. Endo, T. S. Kim, T. Ishihara, Y. Mizushima, M. Higaki, and J. Ito, Drug delivery to the cochlea using PLGA nanoparticles. *Laryngoscope* 115, 2000 (**2005**).

11. A. Mitra, B. R. Nan, H. Line, and H. Ghandehari, Nanocarriers for nuclear imaging and radiotherapy of cancer. *Curr. Pharm. Des.* 12, 4729 (**2006**).

12. F. J. Hass, P. S. Lee, and R. V. Lourenco, Tagging of iron oxide particles with 99mTc for use in the study of deposition and clearance of inhaled particles. *J. Nucl. Med.* 17, 122 (**1976**).

13. T. Banerjee, A. K. Singh, R. K. Sharma, and A. N. Maitra, Labeling efficiency and biodistribution of Technetium-99m labeled nanoparticles: Interference by colloidal tin oxide particles. *Int. J. Pharm.* 289, 189 (**2005**).

14. J. Panyam and V. Labhasetwar, Biodegradable nanoparticles for drug and gene delivery to cells and tissue. *Adv. Drug Deliv. Rev.* 55, 329 (**2003**).

15. R. A. Wassel, B. Grady, R. D. Kopke, and K. J. Dormer, Dispersion of super paramagnetic iron oxide nanoparticles in poly(D,L-lactide-co-glycolide) microparticles. *Colloids and Surfaces A* 292, 125 (**2007**).

16. L. N. Okassa, H. Marchais, L. Douziech-Eyrolles, K. Herve, S. Cohn-Jonathan, E. Munnier, M. Souce, C. Linassier, P. Dubois, and I. Chourpa, *Euro. J. Pharmaceu. Biopharmaceu.* 67, 31 (**2007**).

17. S. Huth, J. Lausier, S. W. Gersting, C. Rudolph, C. Plank, U. Welch, and J. Rosenecker, Insights into the mechanisms of magnetofection using PEI-based magnetofectins for gene transfer. *J. Gene Med.* 6, 923 (**2004**).

18. A. L. Barnes, R. A. Wassel, F. Mondalek, K. Chen, K. J. Dormer, and R. D. Kopke, Magnetic characterization of superparamagnetic nanoparticles pulled through membranes. *Biomagnetic Res. and Technol.* 5, 1 (**2007**).

19. F. G. Mondalek, Y. Y. Zhang, R. Kopke, B. Kropp, and K. J. Dormer, A novel model of the round window membrane in magnetic targeted delivery. *J. Nanobiotechnology* 4, 4 (**2006**).

20. S. Bala, S. Hariharan, and M. N. V. R. Kumar, PLGA nanoparticles in drug delivery: The state of the art. *Crit. Rev. in Therapeutic Drug Carrier Systems* 21, 387 (**2004**).

21. A. Braden, J. Kashyap, J. Vasir, V. Labhasetwar, and J. K. Vishwananatha, Polymeric nanoparticles for sustained down-regulation of Annexin A2 lead to reduction in proliferation and migration of prostate cancer cells. *J. Biomed. Nanotech.* 3, 148 (**2007**).

22. S.-J. Lee, J.-R. Jeong, S.-C. Shin, J.-C. Kim, Y.-H. Chang, K.-H. Lee, and J.-D. Kim, Magnetic enhancement of iron oxide nanoparticles encapsulated with poly(D,L-Lactide-co-glycolide). *Colloids and Surfaces A Physicochem. Eng. Aspects* 255, 19 (**2005**).

23. Y.-M. Yi, T.-Y. Yang, and W.-M. Pan, Preparation and distribution of 5-fluorouracil $^{125}$I sodium alginate-bovine serum albumin nanoparticles. *World J. Gastroentererology* 5, 57 (**1999**).

24. T. M. Sanchez, A. S. Vila, I. Soriano, C. Evora, J. L. Vila-Jato, and M. J. Alonso, The role of PEG on the stability of PEG-PLA nanoparticles following oral administration. *Colloids Surf. B Biointerfaces* 1, 3 (**2000**).

25. R. Rossin, D. Pan, Q. Kai, J. L. Turner, X. Sun, K. L. Wooley, and M. J. Welch, $^{64}$Cu-labeled folate-conjugated shell cross-linked nanoparticles for turmor imaging and radiotherapy: Synthesis, radiolabeling, and biologic evaluation. *J. Nucl. Med.* 46, 1210 (**2005**).

26. M. Hamoudeh, H. Salim, D. Barbos, C. Paunoiu, and H. Fessi, Preparation and characterization of radioactive dihhenium decacarbonyl-loaded PLLA nanoparticles for radionuclide intratumoral therapy. *Eur. J. Pharm. Biopharm.* (**2007**), in press.

27. J. C. Hung, G. A. Wiseman, H. W. Wahner, B. P. Mullan, T. R. Taggart, and W. L. Dunn, Filtered technetium-99m-sulfur colloid evaluated for lymphoscintigraphy. *J. Nucl. Med.* 36, 1895 (**1995**).

28. M. M. Edreira, L. L. Colombo, J. H. Perez, E. O. Sajaroff, and S. G. de Castiglia, *In vivo* evaluation of three different 99mTc-labelled radiopharmaceuticals for sentinel lymph node identification. *Nucl. Med. Commun.* 22, 499 (**2001**).

29. V. D. Awasthi, B. Goins, R. Klipper, and W. T. Phillips, Accumulation of PEG-liposomes in the inflamed colon of rats: Potential for therapeutic and diagnostic targeting of inflammatory bowel diseases. *J. Drug Target.* 10, 419 (**2002**).

30. C.-M. Fu, Y.-F. Wang, Y.-C. Chao, S.-H. Hung, and M.-D. Yang, Directly labeling ferrite nanoparticles with Tc-99m radioisotope for diagnostic applications. *IEEE Trans. Magnetism* 40, 3003 (**2004**).

31. M. Tafaghodi, S. Abolghasem, S. Tabassi, M.-R. Jaafari, S. R. Zakavi, and M. Momen-Nejad, Evaluation of the clearance characteristics of various microspheres in the human nose by gamma-scintigraphy. *Intl. J. Pharmaceutics* 280, 125 (**2004**).

32. L. H. Reddy, R. K. Sharma, K. Chuttani, A. K. Mishra, and R. R. Murthy, Etoposide-incorporated trapalmitin nanoparticles with different surface charges: Characterization, radiolabeling and biodistribution. *The AAPS Journal* 6, 1 (**2004**).

33. S. W. Ziehuis, J.-H. Seppenwoolde, V. A. P. Mateus, C. J. G. Bakker, G. C. Kriger, B. A. Zonnerberg, A. D. Van het Schip, G. A. Koning, and J. F. W. Nijsen, Lanthanide-loaded liposomes for multimodality imaging and therapy. *Cancer Biotherapy and Radiopharmaceut.* 21, 520 (**2006**).

34. N. L. Mills, N. Amin, S. D. Robinson, A. Anand, J. Davies, D. Patel, J. M. de la Fuente, F. R. Cassee, N. A. Boon, W. MacNee, A. M. Millar, K. Donaldson, and D. E. Newby, Do inhaled carbon nanoparticles translocate directly into the circulation in humans? *Am. J. Resir. Crit. Care Med.* 173, 426 (**2006**).

35. M. M. Kleither, D. Yu, L. A. Mohammadian, N. Niehaus, I. Spasojevic, L. Saunders, B. L. Viglanti, P. S. Yamolenko,

M. Hauck, N. A. Petry, T. Z. Wong, M. W. Dewhirst, and D. E. Thrall, A tracer dose of technetium-99-m-labeled liposomes can estimate the effect of hyperthermia on intratumoral doxil extravasation. *Clin. Cancer Res.* 12, 6800 (**2006**).

36. K. H. Park, H. C. Song, K. Na, H. S. Bom, K. H. Lee, S. Kim, D. Kang, and D. H. Lee, Ionic strength-sensitive pullulan acetate nanoparticles (PAN) for intratumoral administration of radioisotope: Ionic strength-dependent aggregation behavior and (99m) Technetium retention property. *Colloids Surf. B Biointerfaces* 24 (**2007**), in press.

37. S. Liang, Y. Wang, J. Yu, J. Xia, and D. Yin, Surface modified superparamagnetic iron oxide nanoparticles: As a new carrier for biomagnetically targeted therapy. *J. Mater. Sci. Mater. Med.* (**2007**), in press.

RESEARCH ARTICLE